STRAIN EVOLUTION DURING COMPRESSION FATIGUE OF BOVINE CANCELLOUS BONE

S. Dendorfer*, H.J. Maier** and J. Hammer*

* Labor für Werkstofftechnik und Metallographie, University of Applied Sciences Regensburg, Regensburg, Germany
** Lehrstuhl für Werkstoffkunde, University Paderborn, Paderborn, Germany

sdendorfer@lwm-regensburg.de

Abstract: Repetitive cyclic loading from daily activities is known to induce fatigue damage and microcracking in bone structures. Local cyclic loading conditions will be even more severe in osteoporotic structures, in pre-damaged skeleton segments and in cases were metallic implants are employed. Whereas for cortical bone, the mechanical behaviour under cyclic loading is sufficiently described, only preliminary data are available for trabecular bone structures. In the present study the deformation behaviour of bovine vertebra trabecular bone specimens is investigated under cyclic loading in compression. A power law relationship was found between the applied normalised load and the number of cycles to failure. A linear decrease of the maximum integral strains at failure with increasing normalised load was observed. Optical deformation measurement of the surfaces indicates that different failure mechanisms are acting in the low-cycle and high-cycle fatigue regimes, respectively. Especially low-cycle fatigue seems to be dominated by transversal strains, which emphasises the need for transverse connections in bone. As the loss of these connections is one main characteristic of osteoporotic structures, a non-proportional reduction in strength at higher loads (low cycle fatigue) may be the result.

Introduction

Fatigue failure is a well known engineering problem in structures that experience cyclic loads [1, 2]. Bones are also exposed to repetitive loads during daily activities, and thus, may fail due to accumulated fatigue damage [3, 4]. It is generally assumed that fatigue induced cracking and crack propagation also promote complex physiological phenomena such as remodelling processes of bones [5]. Such processes allow an adaptation of the bone to the actual loading scenario. Still, in cases where the crack propagation rate exceeds the remodelling velocity, fatal fracture of the bone finally results. Clinically fatigue fractures are known as “stress fractures” and are common amongst athletes and military personal [6] who repetitively exercise similar motions. Damage accumulation due to cyclic loading is reported to weaken vertebrae [3] and is often associated with loosening of implants [7]. In several studies the fatigue behaviour of both cortical [8-14] and cancellous bone was investigated [15-21]. Similar to engineering materials the general fatigue behaviour of bone is found to be characterised by a decrease in fatigue life as cyclic stresses increase, associated with a reduction in stiffness and accumulation of permanent strains during testing. The contribution of creep deformations to the overall fatigue behaviour still remains unclear [19, 20, 22]. Cyclic loading in compression is the most common test method for fatigue analysis of trabecular bone, and normalised loads (σ/E_0) typically vary between near zero and a given maximum value. Micro damage was identified using a fluorochrome staining technique [17]. Deformations were mostly measured using extensometers. In quasi-static and stepwise compression tests, optical methods were used to measure displacements of markers on individual trabeculae near the surface [23]. Recently, three-dimensional image correlation techniques were developed, which use high-resolution computed tomography [24, 25]. Micro finite element analysis have been applied to models, which represent the actual trabecular architecture in order to compute local strain fields [26, 27], and were used to model fatigue damage accumulation in regular and Voronoi honeycomb structures [28, 29]. These sophisticated approaches are rather complex and time consuming, which limits their application with respect to fatigue analyses.

In this study optical deformation analysis was applied to measure the two-dimensional surface strain distribution during compressive fatigue testing. Special emphasis was on the evolution of local strains and their contribution to the integral measured deformation. The regions of initial local strain concentrations were detected and correlated with the damage after catastrophic failure using scanning electron microscopy (SEM).

Materials and Methods

A total of 32 bovine cancellous bone specimens were loaded in compression fatigue at different normalised stress levels. In all tests, rectangular cancellous bone specimens (16 x 7.75 mm²) from bovine lumbar vertebrae [30] were used (six spine segments, age 18-24 month). All vertebrae were fresh frozen at -20 °C. Cores were taken in inferior – superior

ISSN: 1727-1983

direction in the centre of each vertebra. The cores were fixed in a custom made device and ground at low speed (grit size: 1200) After the removal of the upper endplate the specimens were cut using a low-speed saw (Discotom-2, Struers) in order to achieve the recommended 2:1 ratio between length and diameter [31]. Marrow was kept and only the endplates were cleaned. All preparations were done in the frozen state and under permanent water cooling. Microscopic analysis of the specimens surfaces revealed no damage due to the preparation process. The specimens were again frozen at -20 °C. Prior to testing each specimen was fully thawed for five hours in 0.9% NaCl solution (coloured with toluidin blue). Bone mineral density (BMD) was measured along the load axis in 2 mm slices for all specimens using a Stratec XCT-900. A random pattern of acrylic paint was applied right before testing. Specimens were embedded in specimen holders with methylmethacrylat (KEM 15, ATM) in order to reduce end artefact errors [32] and gripped in a servo-hydraulic testing system (MTS 810 System, Teststar II). All fatigue tests were performed under load control at 1 Hz in 37 °C, 0.9% NaCl solution. Deformation was measured on two sides of the specimen with an optical deformation measurement system (Aramis, GOMbh). This setup allowed for a continuous two-dimensional analysis of the surface deformations. The specimens were preloaded to -50 N to ensure full contact [18-20]. Prior to fatigue testing ten cycles from -50 N to -300 N were applied to determine the initial modulus of the specimen. A triangular wave form from -50 N to the prescribed load value was applied until an integral strain of three percent, which is associated with catastrophic failure, was reached. In order to reduce the scatter of the results, applied load was divided by the secant modulus [17, 19, 20] of the fifth cycle (E5). In cases with a low number of cycles to failure, N < 50, the secant modulus of the first cycle was taken. The normalised load ratios σ/E_5 ranged from 0.385 to 1.47 percent. Failure was defined as a ten percent reduction in modulus in order to facilitate comparison with literature data [20].

Normalised loads were correlated with the number of cycles to failure (N_f), integral residual and integral maximum strains. On-axis, longitudinal and perpendicular, transversal strains were analysed and the total area was classified in steps of 1 percent strain bounds from 0 to 5 percent. The percentage of strained area within a certain bound was plotted versus the number of cycles for each specimen. All specimens were merged in a further step by analysing the strained areas at failure and correlating these values with the corresponding normalised load ratios.

The regions where the fatal cracks initiated were detected using the optical deformation measurement system. After an applied total strain of 1.33% five specimens were analysed by scanning electron microscopy (LEO 1455 VP) and damage was correlated with early strain concentrations.

Results

The integral fatigue behaviour of the bovine cancellous bone specimens is characterized by a reduction of the secant modulus, an increasing hysteresis loop width and by accumulated residual strains, which are associated with a shift of the hysteresis along the strain axis. The number of cycles to failure for the 32 specimens ranged from 3 to 570,000. One specimen showed no failure and was stopped at the latter value. Characteristic hysteresis loops for a medium loaded specimen are shown in Figure 1.

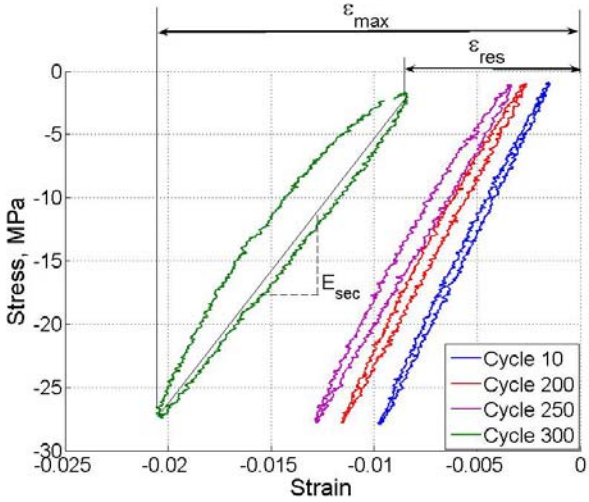

Figure 1: Stress – strain hysteresis loops for a normalized stress of σ/E_5 = 0.0075 for the cycles 10, 200, 250 and 300.

The overall course of a single fatigue test can be classified by three stages: A strong increase of inelastic deformation at the beginning followed by a saturation regime and finally a rapid increase of inelastic deformation, which is associated with macroscopic failure at the end of the test. Merging all experiments, a highly correlated power law between the normalised load ratios and the number of cycles to failure is found:

$$\sigma / E_5 = 0.0133 \times N_f^{-0.0939}, R^2 = 0.905 \qquad (1)$$

By using the average BMD value (0.383 ± 0.867 g/ccm) of each specimen as a scale factor for the applied load ratio a worse correlation was obtained.

Maximum strains at failure (defined as a ten percent reduction in modulus) showed a linear relationship to the normalised load ratio (Figure 2):

$$\varepsilon_{\max} = -1.204 \times (\sigma / E_5) - 0.001368, R^2 = 0.833 \qquad (2)$$

Therefore, higher normalised load ratios correspond to higher integral strains at failure, while lower applied load ratios result in lower maximum strains at failure. A similar, but less well correlated expression was found for the residual strains.

In order to quantify the surface strain distribution, strains within certain bounds were summed and plotted versus the number of load cycles. The bounds employed

ISSN: 1727-1983

are: 1%, 2%, 3%, 4% and 5%. A sensitivity study ensured that the bound values chosen deliver enough accuracy and resolution.

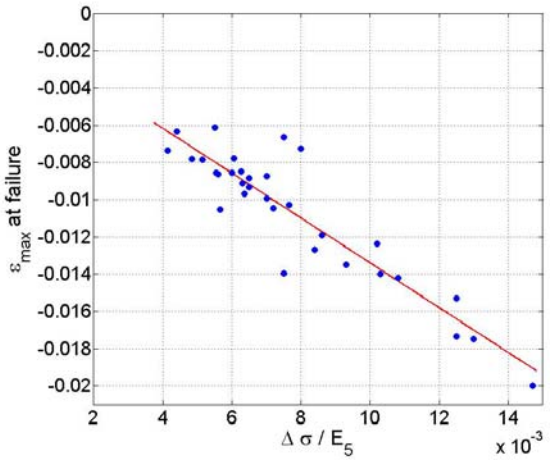

Figure 2: Maximum strains at failure versus normalised load ratio.

In Figure 3 the results for a fatigue test with a normalised load level of 0.0086 are plotted. The strain components are divided in the longitudinal loading direction (LD) and the transversal loading direction (TD). For the sake of clarity only the lower two strain bounds are plotted for both components. The higher strain components are much smaller in magnitude. LD and TD strain components exhibit the same characteristics: The areas of strains within 0 and 1% slightly decrease throughout the whole experiment with a more pronounced decrease near the end of the experiment. The areas of strains within higher bound values behave vice-versa with a slight increase at the beginning of the fatigue test and during the saturated state followed by a more distinct increase close to failure. These effects are much more pronounced in the transversal direction. Additionally, areas with strains over 1% were found with a higher amount in the transversal direction and strains below 1% with a lower amount, respectively.

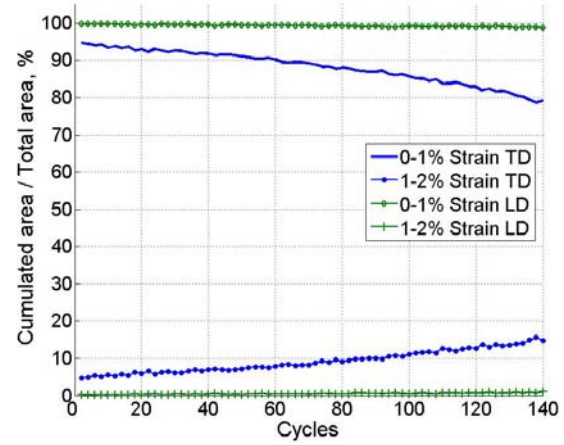

Figure 3: Cumulated areas in percent of total area, strain range 0-1% and 1-2% in transversal direction (TD) and longitudinal, main loading, direction (LD), σ/E_0 = 0.0086.

By analysing the cumulated area fractions within the strain bounds at failure, correlations with the normalised load ratios can be established. The area fractions for the longitudinal loading direction for the lower three strain classes are shown in Figure 4. A lower normalised load ratio results in more areas within higher strain bounds, whereas areas within the first bound (0-1%) are, as direct result of this, less in number. With increasing normalised load level fewer areas with higher strain components were found.

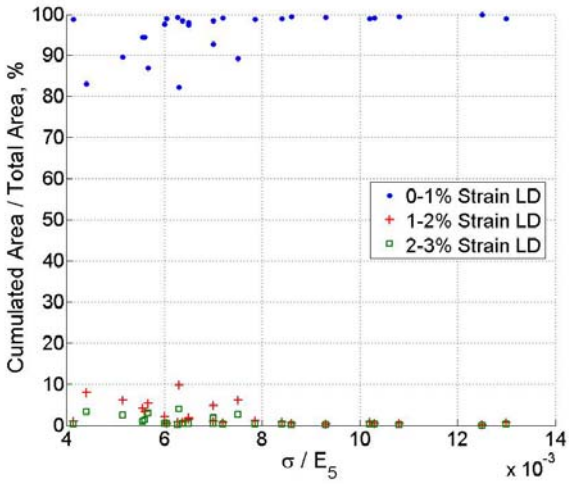

Figure 4: Area fraction within certain strain bounds at failure versus normalised load ratios for longitudinal direction strain components.

The local strain distributions at the surface of a low-loaded specimen are shown in percent values in Figures 5 and 6. Figure 5 shows the strain distribution perpendicular to the loading direction at approximately 18% of the total specimen lifetime. Few distinct areas that display strain concentrations are visible, which are directly related to the architecture of the specimen. Each pair of positive and negative strain components represents the deformation of a cell and its trabeculae, respectively. The von-Mises strain distribution at failure for the same specimen is shown in Figure 6. Only one of the regions that demonstrated significant strain concentration in Figure 5 played a major role in macroscopic failure propagation. The critical 'hot spot' is indicated by the circle.

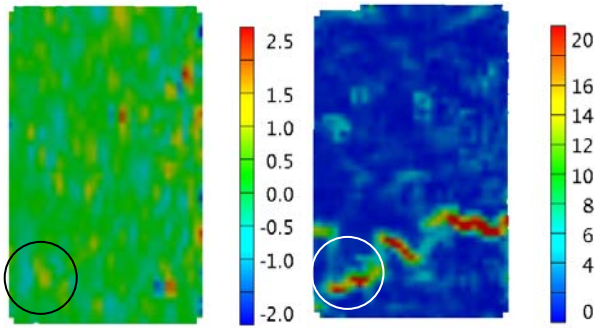

Figure 5: Surface strain distribution (TD) at cycle

Figure 6: Von-Mises surface strain distribution

ISSN: 1727-1983

10,000, $\sigma/E_0 = 0.00414$. at macroscopic failure (cycle 185,000).

Depending on the orientation of the trabeculae, two distinctive failure modes were found in the SEM analysis. The crack initiation in four specimens occurred at trabeculae that were oriented nearly parallel to the in loading direction. In one case crack initiation occurred in a trabecula that was oriented at approximately 45 degrees (Figure 8). The trabecula where macroscopic failure initiated for the specimen shown in Figure 5 is displayed in Figure 7. A shear compression fracture is visible. Another example for a 'hot spot' of failure initiation is shown in Figure 8, the fractured trabecula exhibits compression fracture with a much more fibrous characteristic.

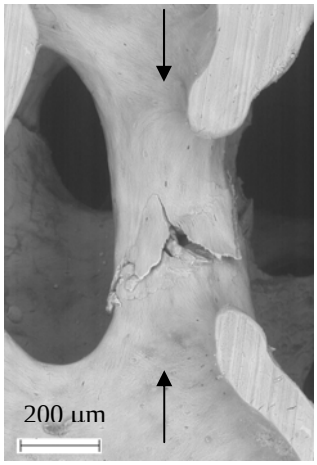

Figure 7: Failure of single trabecula, $\sigma/E_0 = 0.0041$, cycle 185,500 (cf. Fig. 5 and 6).

Figure 8: Failure of a single trabecula, $\sigma/E_0 = 0.0067$, cycle 1,747.

Transversal oriented trabeculae failed preferentially by longitudinal crack formation along the trabecula axis (Figure 9).

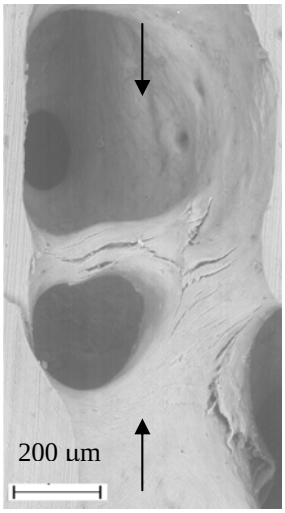

Figure 9: Transversal failure of trabeculae, $\sigma/E_0 = 0.007$, cycle 2,000.

Discussion

The (integral) fatigue behaviour of bovine cancellous bone was found to be, in accordance with literature [18, 19, 33], characterised by a powerlaw relationship of the normalised load and number of cycles to failure, increasing hysteresis loop widths and accumulated residual strains.

Maximum global strains at failure were found to be linearly increasing with increasing normalised load ratio. By contrast, the percentage of areas with local longitudinal strains (at failure) of higher magnitude decreases with an increase of the normalised load ratio. Therefore, the observed higher integral strain at failure is a result of highly concentrated local (LD) deformation in few areas. Lower normalised load ratios lead to more areas with higher strains but integrating the local deformations along the specimen result in a smaller global deformation. This effect seems to be in contrast to earlier findings, were surface von-Mises strains during compressive fatigue were analysed and the areas with strains of a magnitude below 1% appear to decrease with increasing normalised load and areas with higher strains behave vice-versa [34]. The rationale for this is a dominating transversal strain component. The predominance of these transversal strains may be a result of the cell geometry and the structures' architecture, respectively. Longitudinally oriented cells may lead in case of strut failure / bending associated with high loads to high transversal deformations and low longitudinal deformations. This can be illustrated with a rotating strut. In the case of low normalised load ratios trabeculae may deform and fail mainly due to microcrack formation and propagation, which leads to a more buckling type of failure. This results in relatively high (local) longitudinal strains and less transversal strains.

At the onset and during the early stages of the fatigue tests, high local strain concentrations were found. These either propagate and finally link up to macroscopic cracks or remain almost unchanged throughout the test. The reasons for this different behaviour are still not clear and detailed architectural and microstructural analysis will be required.

The microscopic examination of the specimen revealed two major failure modes. Trabeculae almost parallel to the load axis showed compression failure mainly triggered by shear with different characteristics at the failure plane: Brittle, sharp edged cracks (cf. Figure 7) and fibrous compression failure (cf. Figure 8). These differences might be explained with the post-failure load bearing capacities as the tests were stopped at a pre-defined strain level. Trabeculae showing early failure and remaining unloaded due to stress redistributions in the structure exhibit a sharper edged crack plane, whilst trabeculae exposed to prolonged compression induce more damage in the mineralised matrix, which may be associated with the fibrous appearance of the damaged region.

ISSN: 1727-1983

Damage in transversal oriented trabeculae mainly appeared to be of delaminated shear type failure mode, associated with bending loads, with the maximum crack opening in the centre of the trabecula. So far, only five specimens were analysed in the SEM, and thus, more tests are required for a sound statistical analysis.

The fatal crack was found to initiate at trabeculae that are oriented almost parallel to the longitudinal direction (cf. Figure 5-7). Similar features were observed in the interior of the specimen, which indicates a minor 'edge effect' of the rectangular specimen geometry. Relatively high local strains in the transversal direction were found at early stages of the experiment, which are directly correlated to bending and/or buckling of the trabeculae. The two main parameters which affect this deformation are the magnitude of the local load on the trabecula and the level of imperfection of the loaded system, which results in bending moments on the trabecula. As this level of imperfection is, amongst others, a function of the length of the trabecula (in terms of Euler loads), the number of transversal trabeculae is of pronounced interest. This fact is especially remarkable because the loss of these transversal connections is one of the main structural degradation effects of osteoporosis [35]. As failure in highly loaded specimens appears to be dominated by longitudinal strains, a consequence of osteoporosis may be a non-proportional lower resistance against high load impacts.

However, the main limiting factor of every in vitro study on bone specimens is that no remodelling processes are included in the experiments. This mechanobiological answer to the loading can be expected to improve the fatigue life by repairing microcracks or in the worst case even deteriorate the situation when the osteoclastic activities interact with fatigue damage.

The focus of further studies will be on the fatigue behaviour of cancellous bone with special emphasis on architectural and structural measures, especially for osteoportic bone.

Conclusions

Bovine cancellous bone specimens were loaded in compression fatigue. The evolution of surface strains was correlated with integral deformation and structural damage. The findings hint to different failure modes in low-cycle and high-cycle fatigue. Failure under low normalised load ratios (HCF), seem to be dominated by microcracking, whereas in the case of high normalised load ratios (LCF), localised failure of struts occurs.

References

[1] SURESH, S. (1998):'Fatigue of Materials', University Press, Cambridge
[2] RADAJ, D. (2003):'Ermuedungfestigkeit', Springer Verlag, Heidelberg
[3] BURR, D. B., FORWOOD, M. R., FYHRIE, D. P., MARTIN, R. B., SCHAFFLER, M. B. AND TURNER, C. H. (1997):'Bone microdamage and skeletal fragility in osteoporotic and stress fractures', J Bone Miner Res, **12**, p. 6-15
[4] MARTIN, R. B., BURR, D.B., SHARKEY, N.A. (1998):'Skeletal Tissue Mechanics', Springer Verlag, New York
[5] PRENDERGAST, P. J. AND TAYLOR, D. (1994):'Prediction of bone adaptation using damage accumulation', J Biomech, **27,** p. 1067-76
[6] MILGROM, C., GILADI, M., SIMKIN, A., RAND, N., KEDEM, R., KASHTAN, H., STEIN, M. AND GOMORI, M. (1989):'The area moment of inertia of the tibia: a risk factor for stress fractures', J Biomech, **22,** p. 1243-8
[7] BAUER, T. W. AND SCHILS, J. (1999):'The pathology of total joint arthroplasty.II. Mechanisms of implant failure', Skeletal Radiol, **28,** p. 483-97
[8] CALER, W. E. AND CARTER, D. R. (1989):'Bone creep-fatigue damage accumulation', J Biomech, **22,** p. 625-35
[9] CARTER, D. R. AND CALER, W. E. (1983):'Cycle-dependent and time-dependent bone fracture with repeated loading', J Biomech Eng, **105,** p. 166-70
[10] CARTER, D. R., CALER, W. E., SPENGLER, D. M. AND FRANKEL, V. H. (1981):'Fatigue behavior of adult cortical bone: the influence of mean strain and strain range', Acta Orthop Scand, **52,** p. 481-90
[11] CARTER, D. R., CALER, W. E., SPENGLER, D. M. AND FRANKEL, V. H. (1981):'Uniaxial fatigue of human cortical bone. The influence of tissue physical characteristics', J Biomech, **14,** p. 461-70
[12] CURREY, J. D. (1988):'Strain rate and mineral content in fracture models of bone', *J Orthop Res*, **6,** p. 32-8
[13] PATTIN, C. A., CALER, W. E. AND CARTER, D. R. (1996):'Cyclic mechanical property degradation during fatigue loading of cortical bone', J Biomech, **29,** p. 69-79
[14] FLECK, C. AND EIFLER, D. (2003):'Deformation behaviour and damage accumulation of cortical bone specimens from the equine tibia under cyclic loading', J Biomech, **36,** p. 179-89
[15] MOORE, T. L. AND GIBSON, L. J. (2002):'Microdamage accumulation in bovine trabecular bone in uniaxial compression', J Biomech Eng, **124,** p. 63-71
[16] BOWMAN, S. M., KEAVENY, T. M., GIBSON, L. J., HAYES, W. C. AND MCMAHON, T. A. (1994):'Compressive creep behavior of bovine trabecular bone', J Biomech, **27,** p. 301-10
[17] MOORE, T. L. AND GIBSON, L. J. (2003):'Fatigue microdamage in bovine trabecular bone', J Biomech Eng, **125,** p. 769-76
[18] MOORE, T. L. AND GIBSON, L. J. (2003):'Fatigue of bovine trabecular bone', J Biomech Eng, **125,** p. 761-8
[19] MOORE, T. L., O'BRIEN, F. J. AND GIBSON, L. J. (2004):'Creep does not contribute to fatigue in bovine trabecular bone', J Biomech Eng, **126,** p. 321-9
[20] BOWMAN, S. M., GUO, X. E., CHENG, D. W., KEAVENY, T. M., GIBSON, L. J., HAYES, W. C. AND MCMAHON, T. A. (1998):'Creep contributes

ISSN: 1727-1983

to the fatigue behavior of bovine trabecular bone', J Biomech Eng, **120,** p. 647-54
[21] RAPILLARD, L., CHARLEBOIS, M. AND ZYSSET, P. K. (2005):'Compressive fatigue behavior of human vertebral trabecular bone', J Biomech, in press
[22] YAMAMOTO, E., PAUL CRAWFORD, R., CHAN, D. D. AND KEAVENY, T. M. (2005):'Development of residual strains in human vertebral trabecular bone after prolonged static and cyclic loading at low load levels', J Biomech, in press
[23] ODGAARD, A. AND LINDE, F. (1991):'The underestimation of Young's modulus in compressive testing of cancellous bone specimens', J Biomech, **24,** p. 691-8
[24] NAZARIAN, A. AND MULLER, R. (2004):'Time-lapsed microstructural imaging of bone failure behavior', J Biomech, **37,** p. 55-65
[25] VERHULP, E., VAN RIETBERGEN, B. AND HUISKES, R. (2004):'A three-dimensional digital image correlation technique for strain measurements in microstructures', J Biomech, **37,** p. 1313-20
[26] VAN RIETBERGEN, B., MULLER, R., ULRICH, D., RUEGSEGGER, P. AND HUISKES, R. (1999):'Tissue stresses and strain in trabeculae of a canine proximal femur can be quantified from computer reconstructions', J Biomech, **32,** p. 443-51
[27] NIEBUR, G. L., FELDSTEIN, M. J., YUEN, J. C., CHEN, T. J. AND KEAVENY, T. M. (2000):'High-resolution finite element models with tissue strength asymmetry accurately predict failure of trabecular bone', J Biomech, **33,** p. 1575-83
[28] SCHAFFNER G., G., X.-D. E., SILVA M. J., GIBSON L. J. (2000):'Modelling fatigue damage accumulation in two-dimensional Voronoi honeycombs', International Journal of Mechanical Sciences, **42,** p. 645-656
[29] GUO, X. E., MCMAHON, T. A., KEAVENY, T. M., HAYES, W. C. AND GIBSON, L. J. (1994):'Finite element modeling of damage accumulation in trabecular bone under cyclic loading', J Biomech, **27,** p. 145-55
[30] SMIT, T. H. (2002):'The use of a quadruped as an in vivo model for the study of the spine - biomechanical considerations', Eur Spine J, **11,** p. 137-44
[31] KEAVENY, T. M., BORCHERS, R. E., GIBSON, L. J. AND HAYES, W. C. (1993):'Trabecular bone modulus and strength can depend on specimen geometry', J Biomech, **26,** p. 991-1000
[32] KEAVENY, T. M., PINILLA, T. P., CRAWFORD, R. P., KOPPERDAHL, D. L. AND LOU, A. (1997):'Systematic and random errors in compression testing of trabecular bone', J Orthop Res, **15,** p. 101-10
[33] MICHEL, M. C., GUO, X. D., GIBSON, L. J., MCMAHON, T. A. AND HAYES, W. C. (1993):'Compressive fatigue behavior of bovine trabecular bone', J Biomech, **26,** p. 453-63
[34] DENDORFER, S., MAIER, H. J. AND HAMMER, J. (2005):'Deformation behaviour of bovine cancellous bone', Proc. of Applied Biomechanics Regensburg, 2005, Germany, accepted

ISSN: 1727-1983